2017 Insensitive Munitions & Energetic Materials Technology Symposium
Double Tree by Hilton Portland, Portland, OR, USA, April 23-26, 2018

Filling the Gap between the Initiation Behavior of Shaped Charge Jets and Fragments

Werner Arnold[1], Thomas Hartmann[2], Ernst Rottenkolber[2]

[1] MBDA-TDW Gesellschaft für verteidigungstechnische Wirksysteme mbH, Hagenauer Forst, D-86529 Schrobenhausen, Germany,
[2] NUMERICS GmbH, Mozartring 6, D-85238 Petershausen, Germany

Abstract

In the previous IMEMTS paper [10] the findings showed that for shaped charge jet (SCJ) attacks the critical stimulus $S = v^2 \cdot d$ (v = jet velocity; d = jet diameter) for the initiation of a munition is no longer constant ($S \neq$ const.) an therefore a new initiation model is necessary. In this work the initiation scope should be extended from SCJs to fragments represented by STANAG projectiles. The original STANAG projectile with L/D = 1 and elongated ones with L/D = 3 made out of steel and copper were shot with a EMI powder gun against the TDW standard charge with the PBX KS32 (HMX/PB 85/15, ρ = 1.64 g/cm³). The results were in good agreement with those achieved during the SCJ trials. A new linear initiation model was proposed: $v = A - B \cdot d$.

1 Introduction

During more than one decade of studying initiation phenomenology numerous papers at previous IMEMTS and other symposia ([1] - [11]) were published. Most of them dealt with the hypervelocity impact initiation of plastic bonded high explosive charges by shaped charge jets (SCJ) and a few ones reported results in the ordnance velocity impact regime with STANAG projectiles [9] and explosively formed projectiles (EFP) [2]. A recent finding of our investigations of charge jet (SCJ) attacks suggests that the critical stimulus $S = v^2 \cdot d$ (v = SCJ / projectile velocity; d = SCJ / projectile diameter) for the initiation of a munition can no longer be seen as a constant ($S \neq$ const.) Also, known equations, e.g. Jacobs-Roslund, are not capable to describe low velocity and hypervelocity impacts with the same parameter set.

Consequently, a new initiation model is needed taking these findings into account. The presented study shall therefore continue the investigations already launched in [10] under the title “Towards a Unified Initiation Model”. On the way to such a new unified model further work has to be done trying to realize a “unifying link” between the initiation phenomenology of shaped charge jet impacts (in the hypervelocity regime) and of projectile impacts (in the lower velocity regime). The situation of today is that a larger number of experimental results are available in the hypervelocity regime of the SCJs and only a few ones in the lower velocity regime of STANAG / EFP projectiles. Therefore, a series of trials were planned and conducted to close the data gap in the low velocity regime.

2 From Shaped Charge to Fragments

For fragments the STANAG projectile is representative according to [12]. While making the transition from SCJ towards STANAG projectile impacts several changes of initiation phenomena are expected. This transition process starts from a continuous copper jet and ends up with the standard steel STANAG projectile with L/D = 1. The individual steps include:

- continuous Cu liner SCJ with velocity gradient
- particulated Cu liner SCJ with different jet particle velocities
- modified STANAG projectile: elongated (L/D > 1) and material changed to Cu
- modified STANAG projectile made of steel but elongated (L/D > 1)
- standard steel STANAG projectile (L/D = 1)

In the first step from a continuous to a particulated (Cu liner) SCJ a first change in the initiation phenomenology could be observed [10]: the second SCJ particle (and all the following ones) now hits moving, but bare high explosive (KS32) leading to a higher sensitivity (larger ERL). Taking the next step, only one elongated (L/D > 1) Cu projectile will be hitting the test charge instead of multiple SCJ particles. Then the next step towards the L/D = 1 STANAG steel projectile makes the transition from Cu to steel, and the final step is done when using an original STANAG steel projectile [12] with L/D = 1. Such a short projectile can erode very quickly while perforating the charge. This might lead to a higher required velocity to initiate the charge, as the initiation now - due to the quick erosion process - must take place at the entry side of the charge (instead of exit side). In any case an at least partial transition from a *penetration mode* to an *impact mode* initiation [4] must occur, which might be accompanied by a further change in required particle velocity.

This short summary of the initiation phenomena induced by the transition from SCJs towards STANAG projectiles already shows that it is not fully clear or foreseeable what will happen when this transition is actually executed. Therefore, further experimental trials with original STANAG-projectiles (L/D = 1 [12], Figure 1 top) and elongated ones made out of steel and copper were planned and conducted. The experimental work was supported by numerical simulations. Like in earlier tests (e.g. [10]) the so called “standard charge” filled with the TDW insensitive high explosive KS32 (HMX/PB 85/15, ρ = 1.64 g/cm³) was used in the investigations (Figure 1 bottom). The charge consists of a high explosive cylinder with 100 mm in diameter and 200 mm in length and a mild steel casing with 10 mm thickness and two screwed lids on both sides (standard threats).

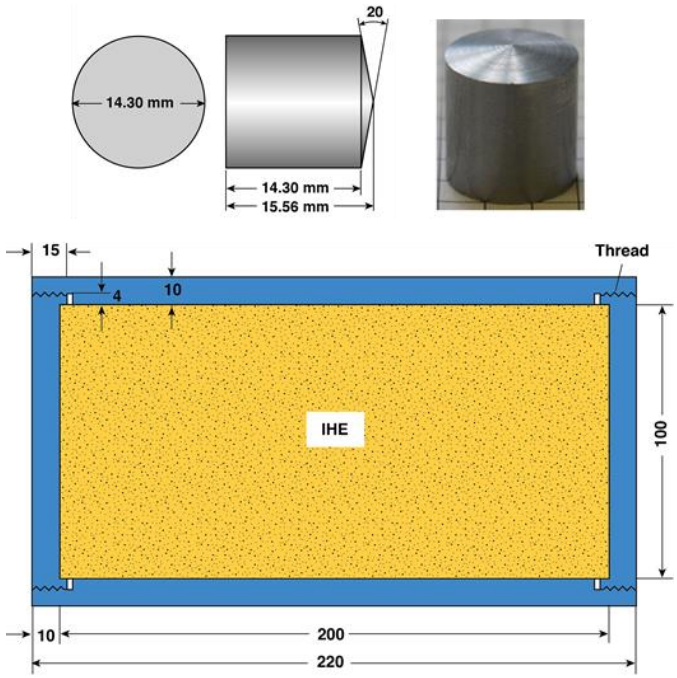

Fig. 1: Original STANAG-projectile (L/D = 1, top) and TDW standard charge (bottom).

3 Numerical Simulations

Numerical simulations were applied to determine the minimum projectile length required to perforate the complete charge and to investigate the erosion process, the velocity reduction during the penetration of the charge, acceptable maximum yaw angle (< 6°), impact velocity vs. projectile velocity behind the steel casing, casing materials etc. The original STANAG projectile (L/D = 1) and elongated ones (L/D = 2, 2.5 & 3) were studied (Figure 2). Besides steel projectiles (in accordance with [12]) also Cu projectiles (making the link to copper SC jets) were regarded. The high explosive was modelled with an inert PBX-simili.

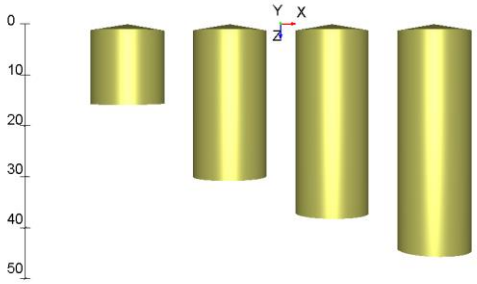

Fig. 2: Simulation models of the STANAG projectile (L/D = 1) and elongated ones (L/D = 2, 2.5 & 3).

A sequence of the penetration of an elongated Cu-projectile (L/D = 3) is shown in Figure 3. The impact velocity (on the steel casing) was 2000 m/s. After perforation of the 10 mm thick steel casing of the charge the projectile is already strongly eroded (ca. 40%). When arriving at the middle of the penetration velocity is close to 1000 m/s. In the simulation the length of the projectile is sufficient to reach the rear side of the charge but it is fully eroded and cannot completely perforate the casing.

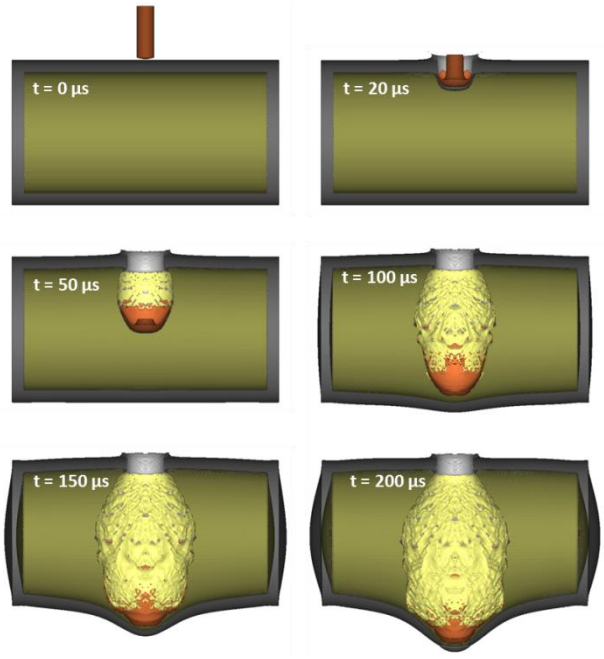

Fig. 3: Sequence from (0 – 200 µs) of the penetration of an elongated Cu-projectile (L/D = 3).

4 Experimental Trials

Figure 4 shows all results of the trials with shaped charges with calibers ranging from 44 mm up to 200 mm (taken from [10]) against the standard charge carried out over the last years.

On abscissa, the parameter *velocity* is used instead of the *stimulus* $S = v^{2} \cdot d$ as done in [10]. This is because the stimulus seems inappropriate as a ranking parameter when comparing ERL results of SCJ vs. STANAG-projectiles, which will be discussed later. On the ordinate the ERL (Explosive Reaction Level) is plotted describing the change in reactivity of the charge when the projectile velocity is increased. A definition of the six ERLs is given e.g. in [10]. The conducted tests shall now add curves for STANAG-projectiles to the chart and thus fill the missing gap between these two most important threats.

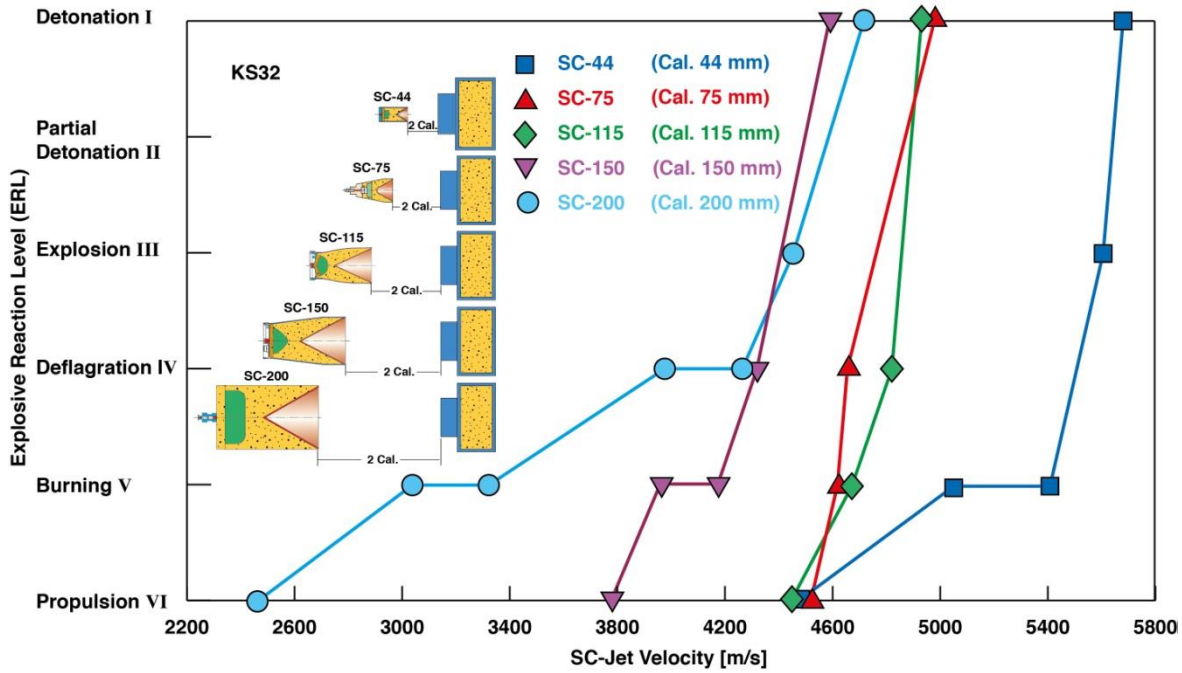

Fig. 4: ERL-curves of all investigated shaped charges (SC) with calibers from 44 mm up to 200 mm (from [10]).

4.1 Test Setup

Firing tests with STANAG-projectiles and their derivatives: L/D = 1 & 3, made from steel and copper materials were planned and carried out. The trials were conducted at the Fraunhofer Ernst-Mach-Institute (EMI) in Germany. A powder gun was used by the EMI to accelerate the projectiles. The projectiles were mounted into a standard sabot which was stripped-off before hitting the target. The upper velocity limit was about 2600 m/s. The larger two-stage light-gas gun (LGG) allowing much higher velocities was out of operation at that time.

The test setup was designed to be as close as possible to the setup used for the SCJ trials (see e.g. [10]). The pictures in Figure 5 (taken at the EMI impact chamber) illustrate the set-up. The projectile enters the chamber through the opening on the left. A high-speed video camera records the projectile´s flight path and permits to determine the impact velocity, the projectile pitch and the impact point on the charge. A mirror is applied to observe the shot from an orthogonal direction and to control projectile yaw. The Aluminum witness plate (2 mm thick) in the background is used to detect higher ERL levels (ERL = I & II). For the lower level reactions, the casing fragments and the KS32 residues respectively were collected and used for the ERL assessment as in the SCJ trials e.g. in [10]. The close-up on the right of Figure 5 shows the TDW standard charge mounted in the projectile´s shot line.

Fig. 5: Test setup at the EMI impact chamber (left) and a close-up of the TDW standard charge (right).

4.2 Test Results

Most tests were performed with the elongated STANAG-projectiles with L/D = 3 with steel and copper materials and it was intended to shoot complete ERL curves with these projectiles. Unfortunately, the maximum velocity reached with the EMI powder gun (v_{max} = 2600 m/s) was too low to achieve a partial or full detonation (ERL = II or I) of the insensitive KS32. Therefore, these parts of the ERL curve had to be assessed by extrapolation. Within the available budget frame, it was not possible to conduct additional trials. However, to get at least an impression of what will happen when taking the last step in the above mentioned transition process, also one shot with the original STANAG L/D = 1 steel projectile was carried out.

4.2.1 Elongated STANAG L/D = 3 Steel and Copper Projectiles

The two diagrams in Figures 6 and 7 for steel and copper projectiles respectively were achieved by incrementally increasing the impact velocities. The impact velocities v_0 were measured with the EMI high speed camera and the ERL were assessed as described above. The photo insets (with respective test numbers) give a vivid illustration of the reaction behavior of the standard charges. In all tests, the impact angles were below the allowable maximum of 6° determined in the numerical simulations (see above).

The reaction behavior of the TDW standard charge with KS32 was mostly the same as that observed with the SCJ attacks described e.g. in [10]. The reaction levels increase in a stepwise way from low level reactions starting at about 2200 m/s to higher level where the casing breaks up into increasingly smaller fragments. The tests exhibit only marginal differences between steel and copper projectiles with a slight trend to lower velocities for the Cu material projectiles – presumably due to the higher mass (density). Extrapolating the available results, it can be anticipated that an impact velocity of about 2700 m/s will be required to reach a partial or full detonation. The differences between steel and copper projectiles are marginal with a slight trend to lesser velocities for the Cu material projectiles, presumably due to the higher mass (density).

4.2.2 Standard STANAG L/D = 1 Steel Projectile

The result of test with the original STANAG steel projectile is also plotted in Figure 6. As expected a distinctly higher impact velocity than with the L/D = 3 projectile was required to the reach same ERL = V (~2600 m/s compared to ~2400 m/s). This was already shortly discussed in Section 2 in the context of the transition phenomenology. The quicker erosion pro-

cess requires higher projectile velocities at the impact / entry side to cause a reaction. In this context also the potentially enforced transition process from a *penetration mode* to an *impact mode* initiation discussed in [4] must be noted.

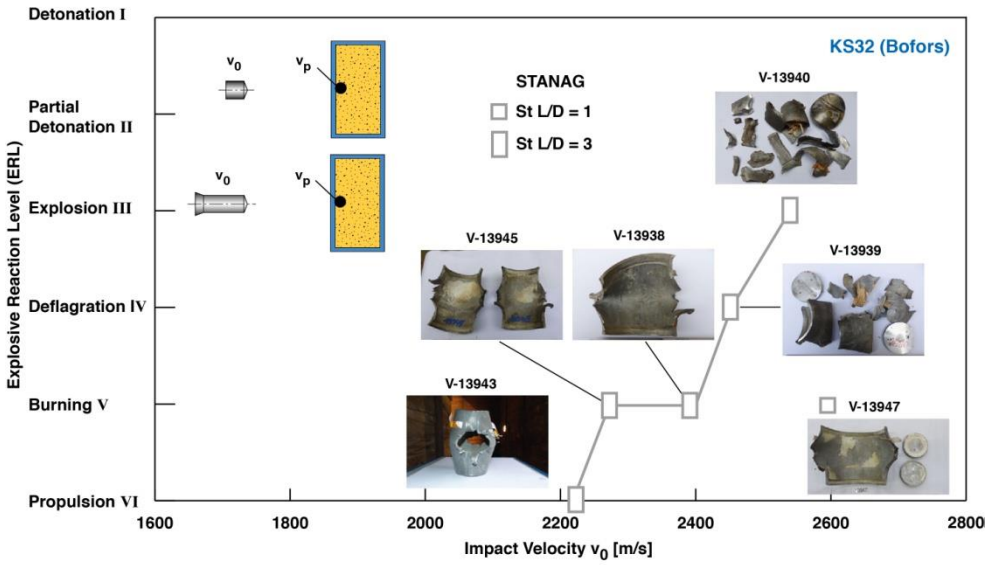

Fig. 6: Test results with steel projectiles with corresponding documentation of the residues.

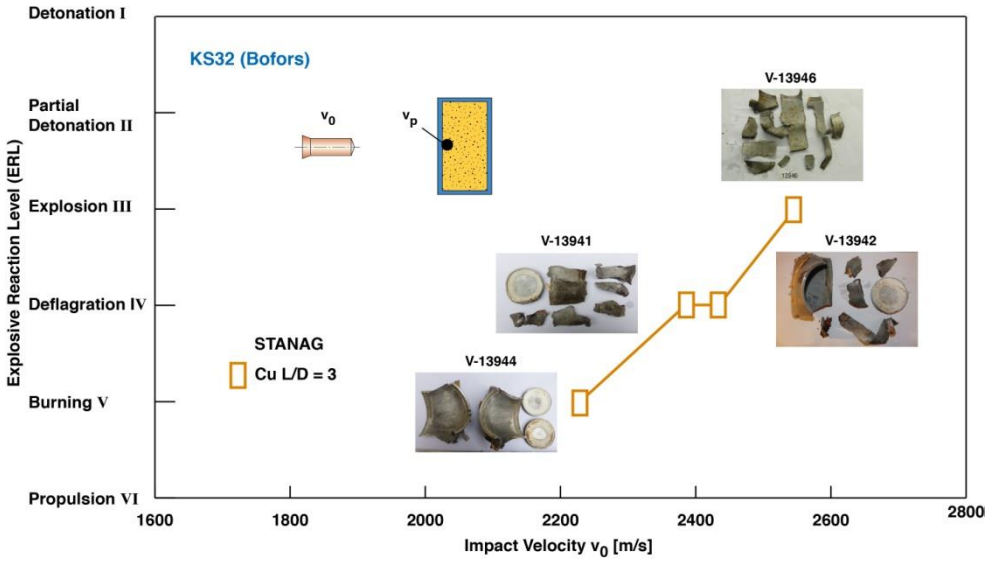

Fig. 7: Test results with copper projectiles with corresponding documentation of the residues.

4.2.3 Initiation Phenomenology

In Section 2, it was assumed that the transition from a *penetration mode* to an *impact mode* initiation process would occur when the projectile aspect ratio is reduced to L/D = 1. The detailed evaluation of the test results indicates that this transition can be already observed with the L/D = 3 projectile. V-13943 with ERL = VI (Figures 6) was found to exhibits a clearly enlarged entry hole, which cannot be observed in the clear *penetration impact mode* situations with shaped charge jets (e.g. [10]). Figure 8 shows the casing after the test and makes clear that this entry hole is much larger and asymmetrical (width 75 mm and height 35 mm) than it could be expected from the STANAG projectile with 14.3 mm diameter. This means

(as numerical simulations showed) that chemical reactions started already at the entry side (characteristic of *impact mode* initiation). On the other hand, also the exit hole is very large (width 90 mm and height 60 mm) seemingly indicating a *penetration mode* initiation.

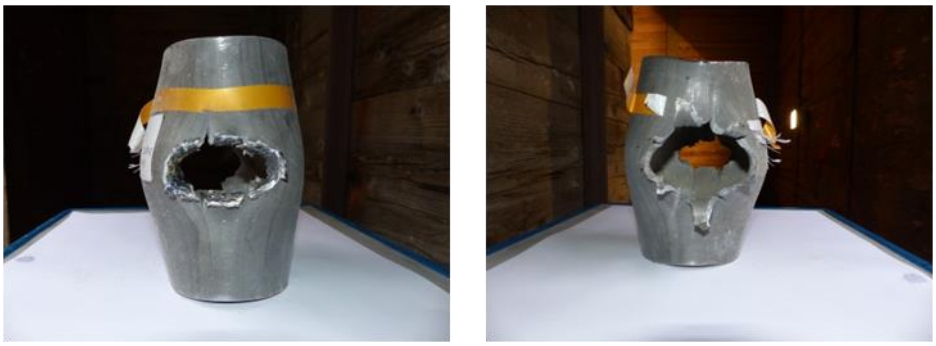

Fig. 8: Steel casing of test V-13943 with ERL = VI: entry side (left) and exit side (right).

4.3 Comparison with SCJ Results

In order to make the STANAG results comparable with the SCJ results in Figure 4 the measured impact velocity v_0 has to be converted to the velocity behind the 10 mm mild steel casing. The result of this transformation is the projectile velocity v_p, at which the projectile is entering the high explosive KS32 and which was used for the SCJ ranking (SCJ velocity behind the barrier). This conversion was accomplished by numerical simulations. Figure 9 exemplarily shows the model setup with an L/D = 3 projectile hitting the steel casing (left) and an L/D = 1 projectile after the perforation (right).

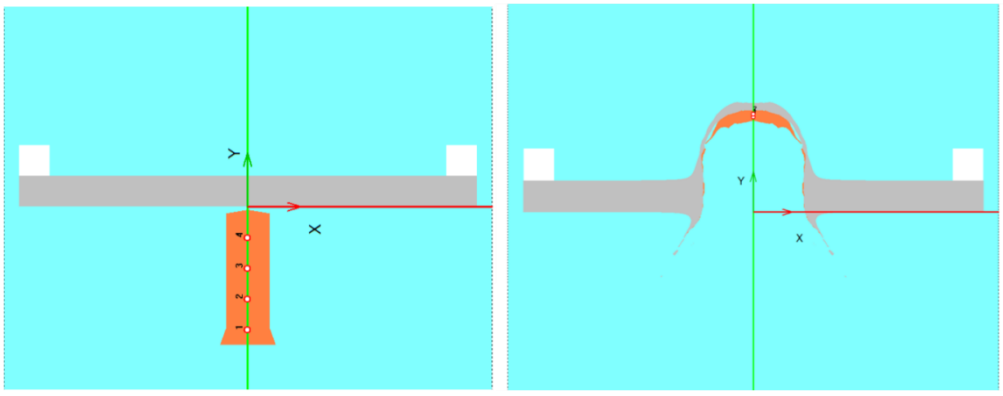

Fig. 9: Model setup: L/D = 3 projectile hitting the steel casing (left).
L/D = 1 projectile after perforation of the steel casing (right).

The diagram in Figure 10 combines all the data of the SCJ trials with those from the STANAG projectile trials. The dashed lines from ERL = III to ERL = I thereby indicate the necessary extrapolation. The STANAG-projectile data fit well in into the overall ERL trends and the data generally look consistent.

It should be noted that this is not at all the case when the ERL is plotted over the stimulus S = v^2d instead of the projectile velocity. In that case the STANAG projectile data would be completely super-positioned with the SCJ data, which would not make sense! Hence, also this result confirms that the stimulus S = $v^2 \cdot d$ is not an appropriate parameter the description of initiation behavior.

Despite the fact that the STANAG data fit in very well there are still a couple of questions that remain unanswered for the moment, e.g.:

- Why are ERL-slopes different between SCJ and STANAG projectile results?
- What is the reason for the ramp-like ERL-slope especially for the SC-200?
- How does the gap between SCJ and STANAG projectile results look like?
- Why does the low velocity of the L/D = 1 steel projectile lead to an ERL = V initiation?
- Is there an influence of the critical diameter of KS32 (d_f ~ 8 mm) being very close to the jet diameter d_j of the SC-200?
- What is the influence of the transition between *impact mode* and *penetration mode* initiation?

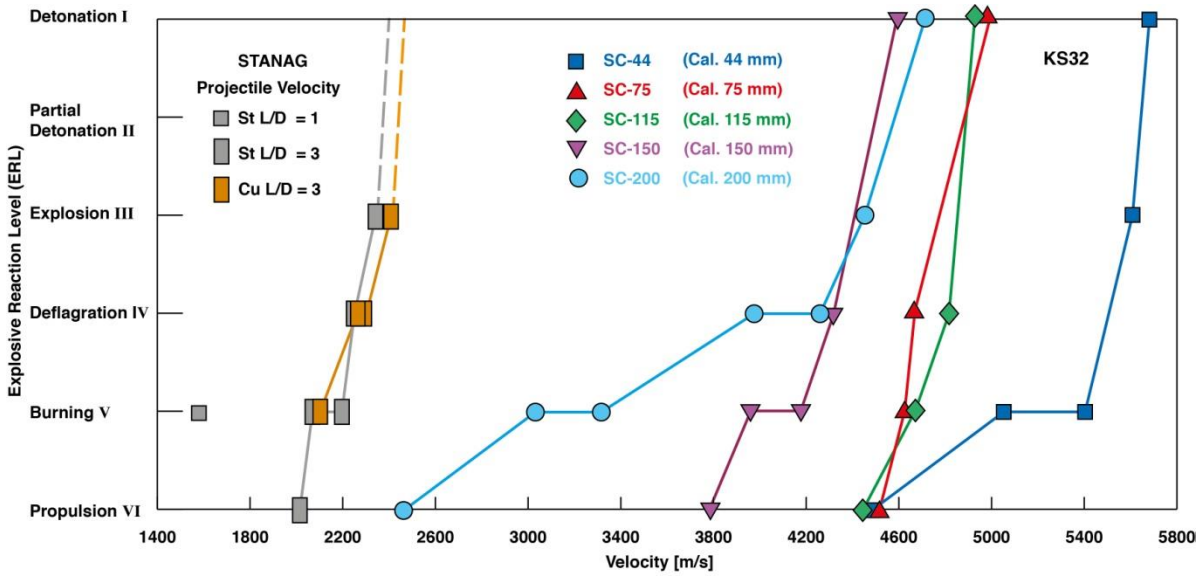

Fig. 10: Comparison of the SCJ results (from [10]) with the STANAG projectile results of this work.

5 New Unified Initiation Model

In [10] it was already realized that the stimulus $S = v^2 \cdot d$ is not an appropriate parameter for description of the observed initiation phenomena. Both parameters v & d (velocity & diameter of the jet / projectile) were used and it was assumed that instead of Eqn. (1) assuming $S = v^2 \cdot d = \text{const} = A^2$:

$$v = A/\sqrt{d} \tag{1}$$

$$v = A - B \cdot d \tag{2}$$

a linear relation as in Eqn. (2) might be a better description.

Using the ERL = I (detonation) and ERL = VI (low reaction / burning) from the data in Figure 10 as upper and lower limit for reactions, the diagram in Figure 11 can be drawn showing such an linear initiation behavior and supporting the proposed formula of (2). Data between the shaped charge SC-200 and the STANAG-projectile are still missing and this gap should be filled up the next years. A first step is already taken in [11].

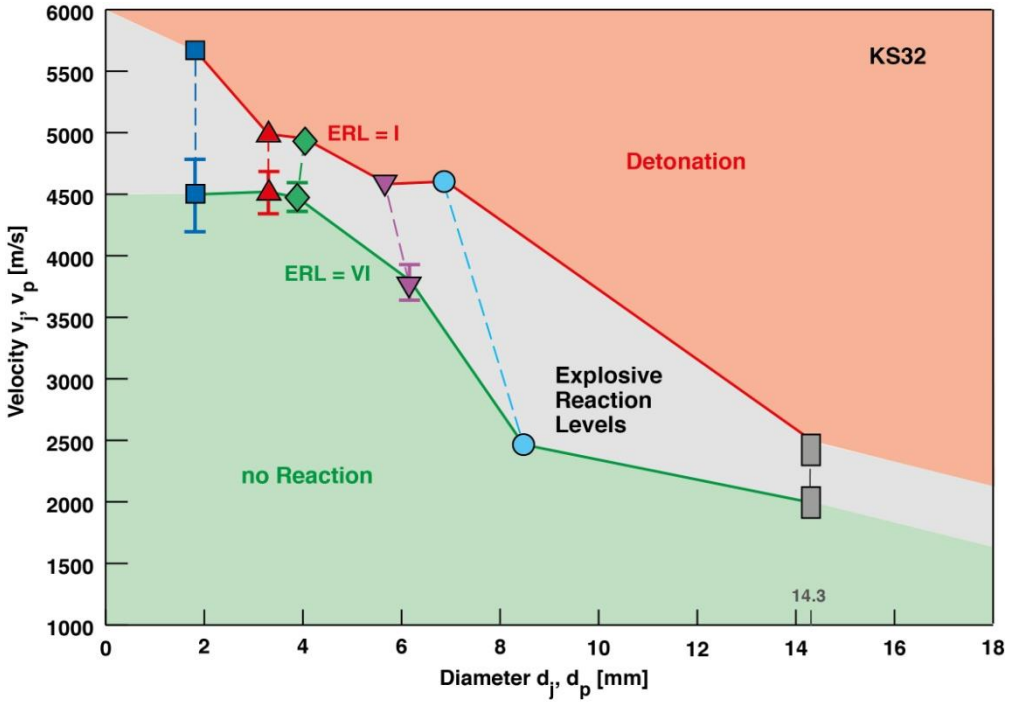

Fig. 11: Approximately linear initiation behavior of the data for ERL = I and ERL = VI.

6 Conclusions

In addition to the numerous initiation trials with SC jets also test campaigns with fragments represented by the STANAG projectile [12] were performed, based on the results achieved in [9]. The conducted experiments were supported by numerical simulations.

Original (L/D = 1) and elongated (L/D = 3) STANAG projectiles made out of steel and copper were shot from the EMI powder gun on the TDW standard charge with the PBX KS32 (HMX/PB 85/15, ρ = 1.64 g/cm³) – the charge already used in the SCJ trials. Since the EMI gun only reached a maximum projectile velocity of about 2600 m/s, the velocity to cause detonation had to be extrapolated and was found to be about 2700 m/s with the elongated projectile.

Obviously a transition process between a *penetration mode* initiation and an *impact mode* initiation [4] was enforced. This could be concluded from the observed reactions at the projectile entry side and from the fact that the L/D = 1 steel projectile erodes very quickly (not being able to reach the exit side of the charge) and requires higher impact velocities.

The new results fit in very well into the already available data set for shaped charge jets (SCJ). Once again the results showed very clearly that the stimulus $S = v^2 \cdot d$ is inappropriate as ranking parameter and that the "S = const. rule" is not valid. The independent parameters v & d (velocity & diameter of the jet / projectile) rather exhibited a linear initiation behavior. Hence, a new initiation model is proposed: $v = A - B \cdot d$.

Acknowledgement

The authors would like to thank the BAAINBw Team K1.2 at Koblenz for the funding of this study and the EMI team at Kandern for conducting the powder gun trials.

References

[1] W. Arnold, E. Rottenkolber, “Sensitivity of High Explosives against Shaped Charge Jets”, Insensitive Munitions & Energetic Materials (IMEMTS) 2007, Miami, USA

[2] W. Arnold, “High Explosive Initiation by High Velocity Pojectile Impact”, HVIS 2010, Freiburg, GE

[3] W. Arnold, M. Graswald, “Shaped Charge Jet Initiation of High Explosives equipped with an Explosive Train”, IMEMTS 2010, Munich, GE

[4] W. Arnold, E. Rottenkolber, “Shaped Charge Jet Initiation Phenomena of Plastic Bonded High Ex-plosives”, IMEMTS 2012, Las Vegas, USA

[5] W. Arnold, E. Rottenkolber, “High Explosive Initiation Behavior by Shaped Charge Jet Impacts”, Hypervelocity Impact Symposium HVIS 2012, Baltimore, USA

[6] W. Arnold, E. Rottenkolber, “Significant Charge Parameters influencing the Shaped Charge Jet Initiation”, IMEMTS 2013, San Diego, USA

[7] W. Arnold, E. Rottenkolber, T. Hartmann, “Analysis of Shock and Jet Initiation Tests of High Explosives”, 15th Int. Symposium on Detonation ISD 2014, San Francisco, USA

[8] W. Arnold, E. Rottenkolber, T. Hartmann, “Challenging v^2d ”, IMEMTS 2015, Rome, IT

[9] W. Arnold, E. Rottenkolber, T. Hartmann, “Testing and Modeling the Initiation of Insensitive Explosives by Projectile Impact”, 11th EUROPYRO International Seminar 2015, Toulouse, France

[10] W. Arnold, T. Hartmann, E. Rottenkolber, “Towards a Unified Initiation Model”, IMEMTS 2016, Nashville, USA

[11] W. Arnold, T. Hartmann, E. Rottenkolber, “Initiation Phenomenology from Hypervelocity to Low Velocity Impacts”, 16th Int. Symposium on Detonation ISD 2018, Cambridge, USA (to be published)

[12] STANAG 4496 (Edition 1), “Fragment Impact, Munitions Test Procedure”, 2006